AD-A045 607 CIVIL AND ENVIRONMENTAL ENGINEERING DEVELOPMENT OFFIC--ETC F/G 13/2
A THEORY ON WATER FILTRATION. PART II. MODEL PRESENTATION.(U)
JUN 77 S P SHELTON
UNCLASSIFIED CEEDO-TR-77-2 NL

| OF |
AD A045607

END
DATE FILMED
11 - 77
DDC

AD A045607

CEEDO-TR-77-2

A THEORY ON WATER FILTRATION
PART II — MODEL PRESENTATION

DET 1,HQ ADTC/ECW
TYNDALL AFB, FL 32403

JUNE 1977

FINAL REPORT FOR PERIOD
JUNE 1973-DEC 1976

CEEDO

Approved for public release; distribution unlimited

CIVIL AND ENVIRONMENTAL
ENGINEERING DEVELOPMENT OFFICE
(AIR FORCE SYSTEMS COMMAND)
TYNDALL AIR FORCE BASE
FLORIDA 32403

UNCLASSIFIED

SECURITY CLASSIFICATION OF THIS PAGE (When Data Entered)

REPORT DOCUMENTATION PAGE

READ INSTRUCTIONS BEFORE COMPLETING FORM

1. REPORT NUMBER (14) CEEDO-TR-77-2	2. GOVT ACCESSION NO.	3. RECIPIENT'S CATALOG NUMBER
4. TITLE (and Subtitle) (6) A THEORY ON WATER FILTRATION - PART II - MODEL PRESENTATION.		5. TYPE OF REPORT & PERIOD COVERED (9) Final rept. 1 Jun 73 - 31 Dec 76
		6. PERFORMING ORG. REPORT NUMBER
7. AUTHOR(s) (10) Stephen P. Shelton Capt, USAF, BSC		8. CONTRACT OR GRANT NUMBER(s)
9. PERFORMING ORGANIZATION NAME AND ADDRESS Det 1 HQ ADTC/ECW Tyndall AFB FL 32403		10. PROGRAM ELEMENT, PROJECT, TASK AREA & WORK UNIT NUMBERS (16) 21036W45 (17) 6W
11. CONTROLLING OFFICE NAME AND ADDRESS Det 1 HQ ADTC Tyndall AFB FL 32403		12. REPORT DATE (11) June 1977
		13. NUMBER OF PAGES 25
14. MONITORING AGENCY NAME & ADDRESS(if different from Controlling Office) (12) 25p.		15. SECURITY CLASS. (of this report) UNCLASSIFIED
		15a. DECLASSIFICATION/DOWNGRADING SCHEDULE

16. DISTRIBUTION STATEMENT (of this Report)

Approved for Public Release; distribution unlimited

17. DISTRIBUTION STATEMENT (of the abstract entered in Block 20, if different from Report)

18. SUPPLEMENTARY NOTES

Available in DDC

19. KEY WORDS (Continue on reverse side if necessary and identify by block number)

Environmental Engineering
Filtration
Mass Transfer
Diffusion
Pressure Drop

20. ABSTRACT (Continue on reverse side if necessary and identify by block number)

The specific objective of this investigation was to apply existing theoretical concepts used in aerosol mechanics to various water filtration systems. Once developed, these equations were used to describe the water filtration processes of concern as a function of the characteristics of the fluid, suspended particles, and filter media. It was concluded that the proposed model had the potential to predict the relationship between flow, pressure, time, and efficiency for the data evaluated. In addition, the model was found to have → next page

DD FORM 1 JAN 73 1473 EDITION OF 1 NOV 65 IS OBSOLETE

UNCLASSIFIED

SECURITY CLASSIFICATION OF THIS PAGE (When Data Entered)

393 250

1B

advantages over current water filtration models since, unlike current models, it considers raw water quality and predicts filtration efficiency.

PREFACE

This report summarizes work between 1 July 1973 and 31 December 1976. Stephen P. Shelton, Capt, USAF, BSC, was the project engineer. This research was preformed under job order 21036W45 at the Air Force Civil Engineering Center.

On 8 April 1977, AFCEC was reorganized into two organizations. AFCEC became part of the Air Force Engineering and Services Agency (AFESA). The R&D function remains under Air Force Systems Command as Det 1 (Civil and Environmental Engineering Development Office (CEEDO)) HQ ADTC. Both units remain at Tyndall AFB, Florida.

This technical report has been reviewed and is approved for publication.

STEPHEN P. SHELTON
Captain, USAF, BSC
Water Quality Research Engineer

PETER A. CROWLEY
Major, USAF, BSC
Director of Environics

DONALD G. SILVA
Lt Col, USAF, BSC
Commander

(The reverse of this page is blank)

TABLE OF CONTENTS

SECTION	TITLE	PAGE
I	INTRODUCTION	1
II	DISCUSSION	2
	REFERENCES	17

LIST OF FIGURES

FIGURE	TITLE	PAGE
1	Logic Flow Diagram for the Proposed Sand Filtration Model	4

LIST OF ABBREVIATIONS, ACRONYMS, AND SYMBOLS

C_t = influent suspended solids concentration

C_{I2} = suspended solids concentration reading the sand layer

D = diffusivity

I = sand bed increment

K_1 = clean filter drag constant

K_2 = filter drag constant with filter cake

K_{2p} = particle drag constant

K_{2s} = sand drag constant

K_D = fluid/media interaction constant

L_C = filter cake thickness

L_S = sand media thickness

ΔP_C = pressure drop across the filter cake

ΔP_I = pressure drop across the Ith sand layer

ΔP_S = pressure drop across the sand media

ΔP_{SA} = total pressure drop through the Ith sand layer

S_f = solidarity factor for filter media

S_t' = solidarity factor for filter cake

T = temperature

$\bar{d}_A$ = arithmetic mean particle diameter

$\bar{d}_e$ = effective particle diameter

$\bar{d}_g$ = geometric mean particle size

$\bar{d}_{AP}$ = arithmetic mean suspended particle diameter

$\bar{d}_{es}$ = effective sand diameter

$\bar{d}_{gp}$ = geometric mean suspended particle size

LIST OF ABBREVIATIONS, ACRONYMS, AND SYMBOLS (CONCLUDED)

$\bar{d}_{mm}$ = mass mean particle diameter

$\bar{d}_{sm}$ = surface mean particle diameter

$\bar{d}_{su}$ = surface mean particle diameter

t = time

μ = approach velocity

η_c = filter cake efficiency

$\eta_{ICD\phi}$ = *modified form of the Friedlander single filter collection efficiency*

$\bar{\eta}_I$ = efficiency of the Ith sand layer

$\bar{\eta}_s$ = total efficiency across the sand media

$\bar{\eta}_{SI}$ = total efficiency through the Ith sand layer

ρ_g = *fluid density*

ρ_p = discrete suspended particle density

ρ_s = sand grain density

ρ_{BP} = particle bed bulk density

ρ_{BS} = sand bed bulk density

σ_s = log normal standard deviation

(The reverse of this page is blank)

SECTION I

INTRODUCTION

This report uses the modified air and water filtration theory from CEEDA-TR-77-1 to develop a common-based rational design sequence for graded media water filters. Characterization of these systems must include terms for all mechanisms having significant influence upon the relationships between flow, time, pressure, and efficiency.

Since the model developed is new, its application to real filtration systems is unknown. Furthermore, the sensitivity of the design variables that characterize the suspended particles in the water is unknown because these data are not used with current water filtration theories. For these reasons a subsequent report will evaluate the model for data sensitivity and accuracy from field data.

SECTION II

DISCUSSION

The model requires information concerning the sand (or other graded media) characteristics, the fluid/particle suspension, and the filter operating conditions. Using these data, the model determines the statistical characteristics of the sand bed and the suspended particles, the effective particle size distribution through the sand bed, the single sand grain collection efficiency, the single suspended particle collection efficiency, and the sand bed solidarity factor. At this point the model integrates numerically to determine the pressure drop caused by the sand, the suspended particles collected in the sand, and the filter efficiency for both the sand and the suspended particles (the cake) at given time increments. In addition, it computes the average efficiency from the start to any point in the filter cycle. The characteristics of the sand bed and the filter cake are then modified for each increment to reflect the net change in their characteristics caused by particles collected during the previous integration increment. Figure 1 is a logic flow diagram of the computer program used to accomplish the above described mathematical sequence. The logic and mathematical expression contained in Figure 1 are discussed herein.

To facilitate a better understanding of the model, input information concerning filter operation includes flow rate per unit area of filter, total filter cycle time, integration increment cycle time (accuracy of the numerical integration technique is inversely proportional to the integration increment), fluid temperature, fluid density, and fluid dynamic viscosity. The design variables requiring definition for the sand bed include mass-mean sand size, log-normal standard deviation of sand size, filter sand bed depth, density of the discrete sand grains, average bulk density of the sand bed, and maximum bulk density of the sand bed.

For a specific sand the mass-mean size, bulk density, maximum bulk density, and discrete sand grain density must be evaluated in the laboratory. These measurements are performed using sieve analysis techniques. The sand size is plotted in percent by mass passing the sieve as a function of sieve size. From these data the remaining particle size distribution variables may be calculated from the mathematical characteristics of a log-normal distribution. A more complete discussion of sieve analysis for filter sands and determination of sand bed characteristics, such as bulk density and discrete sand grain density, has been written by several investigators (References 1-7).

Determination of the characteristics of the suspended particle population is also necessary for the filtration model. The method used to accomplish this may vary according to the particle size range

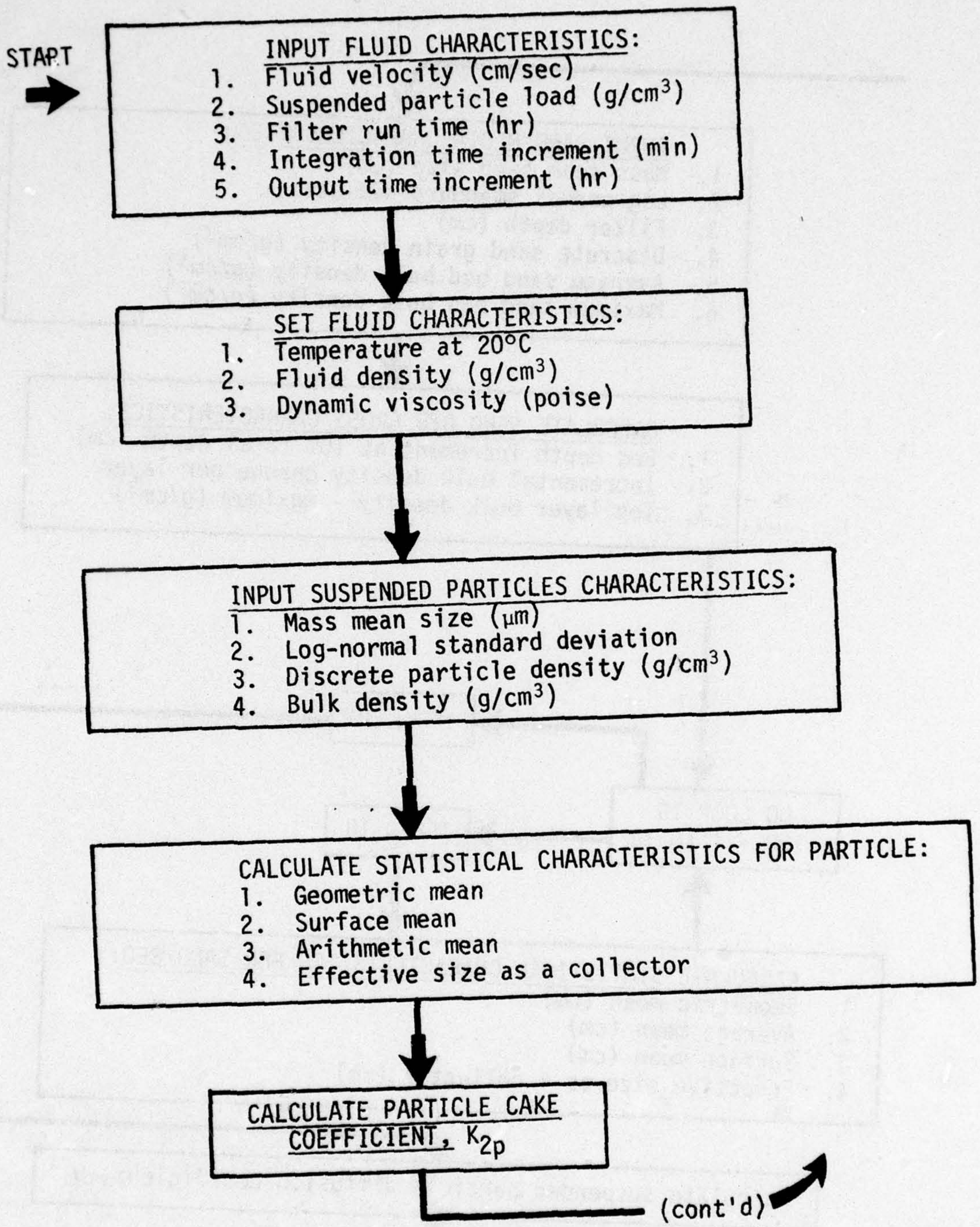

Figure 1. Logic Flow Diagram for the Proposed Sand Filtration Model

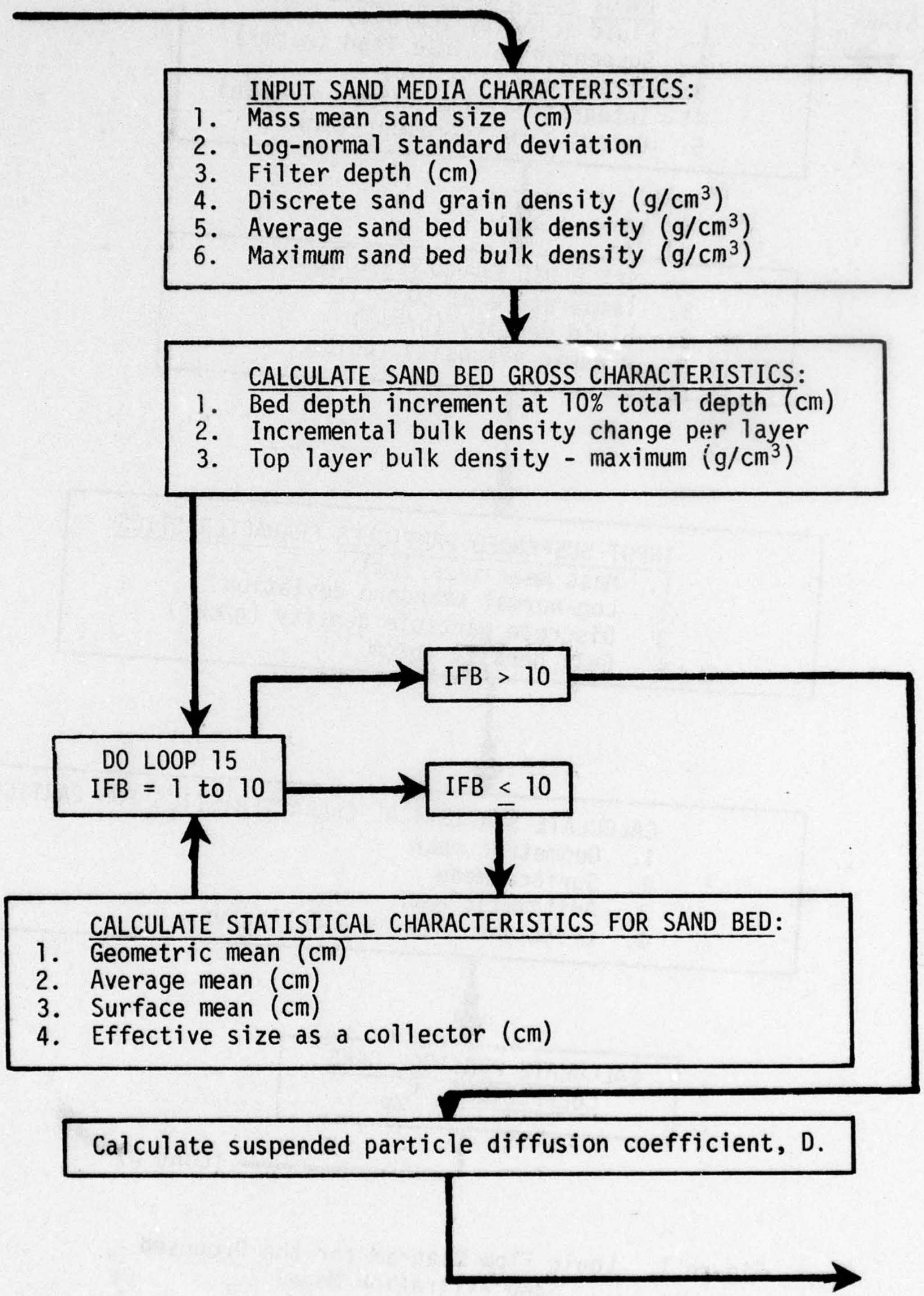

Figure 1. (Continued)

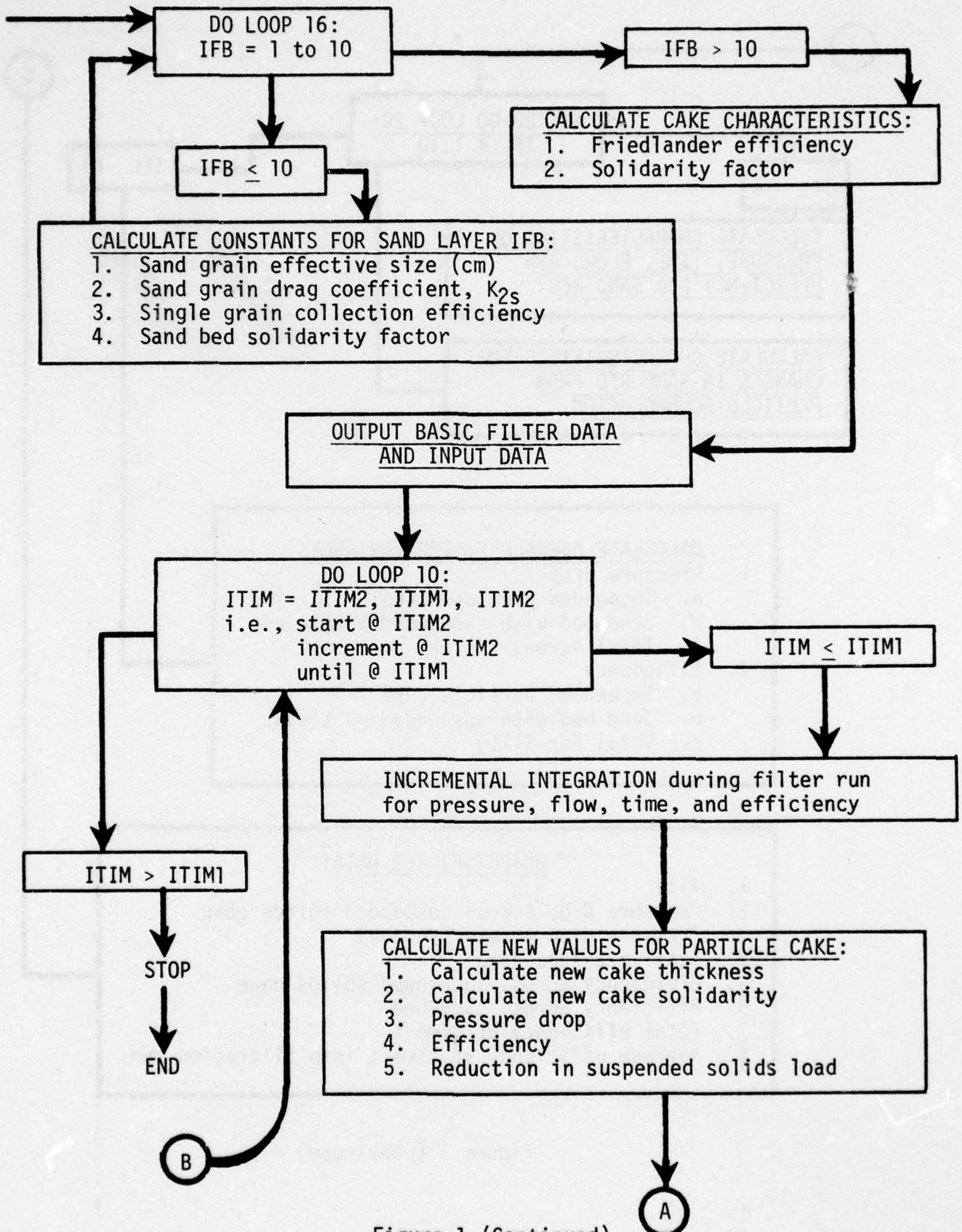

Figure 1 (Continued)

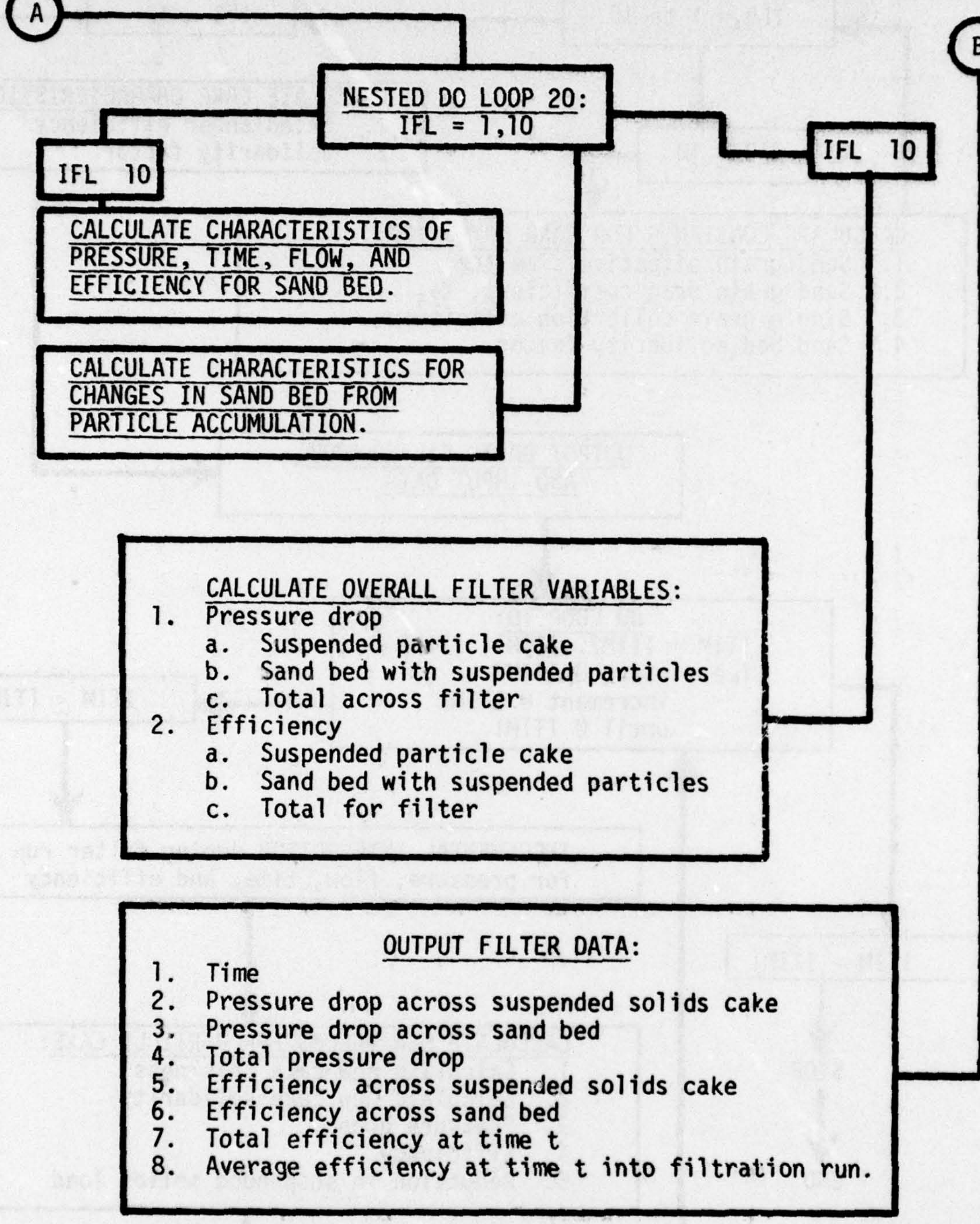

Figure 1 (Concluded)

contained in the population. A primary method for particle size determination could be hydrometric analysis. This method works well for particles as small as 1.0 μm in diameter (Reference 8). Secondary methods such as zonal centrifugation and nuclei counting techniques (Reference 8) may be employed if a substantial mass of the particle population is below 1.0 μm in diameter. Suspended particle bed bulk density and discrete particle density can be determined from gravimetric analysis (Reference 9).

With this information the sand grain or the suspended particle size distribution can be classified. These calculations include determination of geometric mean particle size:

$$\bar{d}_g = \exp[\ln \bar{d}_{mm} - 6.908 \ln^2 (\sigma_g)] \tag{1}$$

where $\bar{d}_g$ is the geometric mean particle size, $\bar{d}_{mm}$ is the mass particle size, and σ_g is the log-normal standard deviation. Next, the surface mean particle size is determined:

$$\bar{d}_{su} = \exp[\ln \bar{d}_{mm} - 1.151 \ln^2(\sigma_g)] \tag{2}$$

where $\bar{d}_{su}$ is the surface mean particle size. The arithmetic mean particle size is then calculated:

$$\bar{d}_A = \exp[\ln \bar{d}_{mm} - 1.263 \ln (\sigma_g)] \tag{3}$$

where $\bar{d}_A$ is the arithmetic mean particle size. When this is accomplished, the effective particle size as a collector is calculated from Chen's (Reference 10) equation:

$$\bar{d}_e = \frac{\bar{d}_{su}^{\,2}}{\bar{d}_A} \tag{4}$$

where $\bar{d}_e$ is the effective particle size for the collector.

At this point, all of the basic input data have been acquired and the basic characteristics of both suspended particles and the sand bed have been calculated (see Figure 1). The first filtration design variable to be calculated is the particle drag coefficient as follows:

$$K_{2p} = \frac{1.84 \times 10^{-3} \rho_{BP}}{\bar{d}_{ep}^2 \, \rho_p{}^2[1 - (\rho_{BP}/\rho_p)]^3} \tag{5}$$

where K_{2p} is the particle drag coefficient (sec/cm), ρ_{Bp} is suspended particle bulk density (g/cm^3), $\bar{d}_{ep}$ is the effective particle size (cm), and ρ_p is the discrete particle density (g/cm^3). The next calculation determines the suspended particle diffusion coefficient. The geometric mean suspended particle size is used for this calculation as suggested by Chen (Reference 10) and Fuchs (Reference 11):

$$D = \frac{1.2096 \times 10^{-17} T}{\mu_g \bar{d}_{gp}} \tag{6}$$

where D is the diffusion coefficient (cm^2/sec), T is temperature (degree Kelvin), μ_g is dynamic viscosity (poise = g/sec·cm), and $\bar{d}_{gp}$ is the geometric mean suspended particle size (cm).

Subsequent to these calculations, the sand bed is divided into ten equal depth increments. The effective sand size, bulk density, filter drag coefficient, single grain collection efficiency, and solidarity factor are determined for each bed depth increment as shown in Figure 1. This is done to account for the gradation occurring when a sand filter is backwashed. The result is effectively constructing a ten-layer sand filter of which each layer is ten percent of the overall sand bed. The effective sand size for each bed increment is determined:

$$\bar{d}_{es}(I) = \exp[\ln \bar{d}_{es} \pm f(I) \ln \sigma_g]$$

where $\bar{d}_{es}(I)$ is the effective sand grain size for bed increment I (cm), $\bar{d}_{es}$ is the average effective sand grain size for the filter (cm), σ_g is the log-normal standard deviation for the sand grain size distribution (cm), and f(I) is the log-normal statistical coefficient. This coefficient has values corresponding to the five through ninety-five percent size, in a log-normal distribution, that permit calculation of the sand grain size that corresponds to the respective percentage using the general form of equation 7.

Because sand that is distributed log-normally in size will settle according to Stokes' law, sand filters exhibit a size gradient from top to bottom. This gradient is created when the sand filter is backwashed and allowed to settle. The large sand grains have a greater terminal velocity than do the smaller grains. For this reason sand grains in the filter bed increase in size from top to bottom. Since particle bed density increases as particle size decreases, the bulk density of the bed decreases from top to bottom. To account for this increase in bulk density, a linear approximation was used in the model between the bulk density of the ten percent size and the average bed bulk density. These two parameters were inputs to the model; the linear approximation calculates the gradient between sand layers and assigns the appropriate bulk density to each layer of the bed.

The filter drag term for each sand layer is calculated:

$$K_{2s}(I) = \frac{1.84 \times 10^{-3}\, \rho_{BS}(I)}{\overline{d}_{es}(I)^2\, \rho_s{}^2\, [1 - (\rho_{BS}(I)/\rho_s)]^3} \tag{8}$$

where $K_{2s}(I)$ is the drag term for sand layer I (sec/cm), ρ_{BS} (I) is the bulk density of sand layer I calculated from the above described linear approximation (g/cm³), $\overline{d}_{es}(I)$ is the effective sand size in sand layer I calculated by equation 7 (cm), and ρ_s is the density of a discrete sand grain (g/cm³). The density of the discrete sand grains is constant for single media filters.

The single grain collection efficiency is determined from the modified Friedlander (References 12, 13) equation; however, for the purposes of this study, the rate of capture was assumed to be unity. The single grain collection efficiency expression may be written:

$$\eta_{ICD\phi}(I) = \left[6\left(\frac{\mu_g}{\rho_g D}\right)^{2/3}\left(\frac{u\,\overline{d}_{es}(I)\rho_g}{\mu_g}\right)^{1/2} + 3\left(\frac{\overline{d}_{AP}}{\overline{d}_{es}(I)}\right)^2\left(\frac{u\,\overline{d}_{es}(I)\rho}{\mu_g}\right)^{1/2}\right]\phi \tag{9}$$

where $\eta_{ICD\phi}(I)$ is the modified Friedlander (References 12, 13) collection efficiency for a single sand grain in bed increment I and ϕ is rate of capture for particles colliding with a sand grain, which is assumed to equal unity.

The last calculation made for the layered filter is the solidarity factor. This is perhaps the most influential parameter in the graded media filter and has been the basis for the development of reverse graded filters in recent years (References 6, 14-18, 20 - 24). As discussed in reference to bulk density, a sand filter media will settle after fluidization with a sand grain size gradient from the top to the bottom of the bed. The grain size increases along this gradient. This is unfortunate because the collection efficiency of a single sand grain is inversely proportional to its size; hence the top layer of sand collects suspended particles most efficiently.

There are two ramifications from this phenomena: (1) because the high efficiency grains make up the upper layers of the media, particles that penetrate the top layer are less likely to be collected in each successive layer and (2) the rapid accumulation of the greatest portion of the suspended particles on the upper sand layer increases the rate of suspended particle formation and hence the rate of increase in pressure drop with time. Under high head-loss situations, the surface of the cake may collapse or the particles, if flocculant in nature, may be crushed. If this occurs, floc break-through may result since the low efficiency lower sand layers may be unable to collect the small particles that have escaped from the upper sand layers and/or the suspended particle cake.

The concept of the reverse graded filter allows the particle size of the graded media to decrease from the top of the filter bed. In this instance greater media penetration can be obtained. Thus the rate of pressure buildup with respect to time, for a given system, should be reduced.

The above discussion emphasizes that the log-normal standard deviation of sand size in a sand filter is a very influential parameter. The uniformity coefficient has long been used in description of filter sand; this term is a rough approximation of the log-normal standard deviation. The solidarity factor for each sand layer is determined from the characteristics of that layer according to the solidarity equation presented previously. This expression may be written:

$$S_f(I) = \frac{0.19099\, L_s\, \rho_{BS}(I)}{\rho_s\, \bar{d}_{es}(I)} \qquad (10)$$

where $S_f(I)$ is the solidarity factor for sand layer I (unitless) and L_s is the overall sand bed depth (cm). As shown in Figure 1, equations 7 through 10 are repeated for each sand layer from the top to the bottom of the sand filter.

After the characteristics of the clean sand filter are established, the characteristics of the suspended particles must be determined. As shown in Figure 1 the first of these characteristics to be determined is the Friedlander equation:

$$\eta'_{ICD\phi} = 6\left[\left(\frac{\mu_g}{\rho_g D}\right)^{-2/3}\left(\frac{u\,\bar{d}_{ep}\,\rho_g}{\mu_g}\right)^{-1/2} + 3\left(\frac{\bar{d}_{AP}}{\bar{d}_{ep}}\right)^{2}\left(\frac{u\,\bar{d}_{ep}\,\rho_g}{\mu_g}\right)^{\frac{1}{2}}\right]\phi' \tag{11}$$

where $\eta'_{ICD\phi}$ is the modified Friedlander (References 12, 13) collection efficiency, $\bar{d}_{ep}$ is Chen's (Reference 10) effective size as a collector (this is calculated using equation 4, using the surface mean suspended particle size and the arithmetic mean suspended particle size; the dimension is cm), $\bar{d}_{AP}$ is the arithmetic suspended particle size (cm), and ϕ' is the probability of a successful attachment upon collision which, for the purposes of this study, is assumed to be unity. At this point in the sequence, it is necessary to make an assumption with respect to the sand/suspended particle interface at the top of the filter. Since the top grains of sand are the smallest in the size distribution, they are assumed to supply the nucleus for suspended particle cake formation. Thus, it is assumed that the surface of the filter is composed of a one-particle-deep layer of suspended solids; the diameter of the particles is equal to the calculated equivalent suspended particle diameter when acting as a collector. Thus, the initial cake solidarity factor is calculated using the effective suspended particle diameter:

$$S'_f = \frac{1.9099\ L_c\ \rho_{BP}}{\rho_p\ \bar{d}_{ep}} \tag{12}$$

where S'_f is the initial solidarity factor of the suspended particle cake (unitless), L_c is the initial cake thickness equal to d_{ep} (cm), the effective particle diameter as a collector according to (Reference 10) equation (cm), ρ_{BP} is the bulk density of the suspended particle cake (g/cm^3), and ρ_p is the density of a discrete suspended particle (g/cm^3).

Once the calculations in equations 1 through 12 are accomplished, numerical integration of pressure, flow, and efficiency as a function of time can be initiated. This is done by incrementing time so that each increment is insignificant with respect to the final accuracy required as shown in Figure 1.

Variables that are affected by the changing characteristics of the filter media, as it accumulates suspended particles on its surface and in the sand itself, are adjusted to reflect this change upon flow, time, pressure, and efficiency during each iteration. These modifications are accomplished sequentially as the graphical integration procedure increments time.

In order to facilitate understanding of the integration incremental sequence, the reader should refer to Figure 1 as its mathematical sequence is described. Suspended particle cake thickness is incremented:

$$L_c(t) = L_c(t-t_I) + \frac{C_I u t_I \eta_c(t-t_I)}{\rho_{BP}} \tag{13}$$

where $L_c(t)$ is suspended particle cake thickness (cm) at time t (sec), $L_c(t-t_I)$ is the suspended particle cake thickness at the previous time increment (t_I is the incrementing unit), $\eta_c(t-t_I)$ is the collection efficiency for the suspended particle cake during the previous time increment, and u is fluid velocity (cm/sec). Once the new cake thickness is determined, $\Delta P_c(t)$ pressure drop caused by the cake (formed from the suspended particles) can be determined:

$$\Delta P_c(t) = K_{2p}\ u\ \rho_{BC}\ L_c(t) \tag{14}$$

where $\Delta P_c(t)$ is the pressure drop caused by the suspended particle cake (g/cm^2) at time t, K_{2p} is the suspended particle unit depth drag coefficient (sec/cm), and $L_c(t)$ is the suspended particle cake thickness at time t.

In addition to the pressure drop, the new solidarity factor for the suspended particle cake can be determined at this point as follows:

$$S_f'(t) = \frac{1.9099\ \rho_{BC} L_c(t)}{\rho_p\ \bar{d}_{ep}} \tag{15}$$

where $S_f'(t)$ is the new suspended particle cake solidarity factor for the increased cake thickness (dimensionless) $L_c(t)$ at time t. At this point the collection efficiency for the suspended particle cake can be calculated:

$$\eta_c(t) = 1 - \exp\left[-S_f'(t)\eta'_{ICD\phi}\right] \tag{16}$$

where $\eta_c(t)$ is the suspended particle cake collection efficiency at time t and $\eta'_{ICD\phi}$ is the modified Friedlander (Reference 12, 13) suspended particle upon suspended particle collection efficiency.

Once the fluid/particle suspension has passed through the particle cake on the surface of the sand media, the concentration of suspended particles in the fluid is reduced by the percent collected. For this reason the suspended particle concentration reaching the top of the sand bed must be calculated:

$$C_{I2} = C_I[1 - \eta_c(t)] \tag{17}$$

where C_{I2} is the suspended solids concentration reaching the sand surface and C_I is the initial suspended solids concentration.

At this point another sequence is necessary to calculate the concentration gradient of the suspended solids in the fluid, as the fluid passes through the sand bed. This is accomplished by determining the mass of solids retained in each sand layer as a function of time. Flow, time, pressure, and efficiency inter-relationships are reevaluated for each successive time increment for all sand layers. The first term calculated in this sequence is the sand layer efficiency:

$$\eta_s(I) = 1 - \exp\left[-S_f(I)\eta_{ICD\phi}(I)\right] \tag{18}$$

where $\eta_s(I)$ is the efficiency, $S_f(I)$ is the solidarity factor, and $\eta_s(I)$ is the efficiency, $S_f(I)$ is the modified Friedlander (11, 12) single grain collection efficiency; all of these are for the I^{th} sand level.

The next calculation predicts the pressure drop across the I^{th} sand level:

$$\Delta P_s(I) = \frac{K_{2S}(I)\ u\ L_s\ \rho_{BS}(I)}{10.} \tag{19}$$

where $\Delta P_s(I)$ is the pressure drop, L_s is the total sand bed depth, $\rho_{BS}(I)$ is the sand bulk density for the I^{th} sand level, and u is filtration velocity.

The next calculation determines the new bulk density of the sand level after suspended particles have been collected during the integration increment. This calculation may be expressed:

$$\rho_{BS}(I)_{ti} = \frac{\rho_{BS}(I) + C_{I2}(I)u\ t_I\ \eta_{ICD\phi}(I)}{(L_s/10.)} \tag{20}$$

where $\rho_{BS}(I)_{ti}$ is the new bulk density for the next time increment, t_I is the time increment, and $\eta_{ICD\phi}(I)$ is the efficiency of the sand layer during the current increment as calculated by equation 18.

Once the new sand bed characteristics of the layer are determined, the filter drag and solidarity factor are modified to consider the accumulated suspended particles. These modifications can be accomplished once the value of the new bulk density, determined by equation 20, is calculated. The other variables affecting the drag coefficient and the solidarity are constant within the integration operation. Filter drag is determined by taking the previous integration increment drag term and adding the drag increase contributed by the newly entrapped suspended particles. This is calculated:

$$K_{2s}(I)_{ti} = K_{2s}(I)\rho_{BS}(I) + \frac{K_{2p}[\rho_{BS}(I)_{ti} - \rho_{BS}(I)]}{\rho_{BS}(I)_{ti}} \tag{21}$$

where $K_{2s}(I)_{ti}$ is the new filter drag term for sand layer I.

The new solidarity factor for the sand layer is determined directly:

$$S_f(I)_{ti} = \frac{1.9099L_s\ \rho_{BS}(I)_{ti}}{10.\ \rho_s\ \bar{d}_{es}(I)} \tag{22}$$

where $S_f(I)_{ti}$ is the new solidarity factor for sand layer I.

Once these modifications are made to the I^{th} layer sand bed characteristics, the values of interest are accumulated. These values include I^{th} level efficiency, pressure drop, and efficiency from the top of the sand bed through the I^{th} level. The efficiency parameter is determined by the accumulation of efficiency as the fluid flows through successive layers of sand. It should be recognized that the accumulation of efficiency terms must express the successive increase as a function of the initial water quality, not as a function of the water quality entering the layer under consideration. For this reason the general addition efficiency expression is written:

$$\bar{\eta}_S = 1 - (1. - \bar{\eta}_{SA})\,(1. - \bar{\eta}_I) \tag{23}$$

where $\bar{\eta}_S$ is the total efficiency from the top of the filter through the I^{th} level, η_{SA} is the total efficiency through the level immediately above the I^{th} level, and $\bar{\eta}_I$ is the efficiency in the I^{th} level.

Unlike efficiency, the total pressure drop at any point in the filter is additive. Thus, the total pressure loss can be expressed:

$$\Delta\bar{P}_S = \Delta\bar{P}_{SA} + \Delta P_I \tag{24}$$

where $\Delta\bar{P}_S$ is the total pressure at the bottom of the I^{th} level, $\Delta\bar{P}_{SA}$ is the total pressure drop through the level immediately above the I^{th} level, and ΔP_I is the pressure drop in the I^{th} level. The last parameter that requires determination in this incremental evaluation of the sand bed is the reduction of the suspended particle concentration through the sand layers above and including the I^{th} sand layer. This is calculated:

$$C_{I2}(I) = C_{I2}\,(1. - \bar{\eta}_s) \tag{25}$$

where $C_{I2}(I)$ is the new suspended solids loading in the fluid after the fluid has passed through layer I and C_{I2} is the suspended particle loading at the top of the sand bed after it has passed through the suspended particle filter cake.

Equations 18 through 25 are repeated through each of the ten sand layers and the values of all parameters are accumulated as prescribed by their respective equation. Once this is accomplished, as indicated by Figure 1, the overall pressure drop and efficiency for the time increment is determined, and the average filtration cycle efficiency is determined. The overall pressure drop is calculated:

$$\Delta P_t = \Delta P_c + \Delta P_s \tag{26}$$

where ΔP_t is the total pressure drop across the filter, ΔP_c is the pressure drop across the suspended particle cake as calculated by equation 14, and P_s is the overall pressure drop across the sand bed as determined by equation 24. The incremental efficiency at any time t is determined:

$$\eta_t(t) = 1. - [1. - \eta_c(t)]\,[1. - \eta_s(t)] \tag{27}$$

where $\eta_t(t)$ is the total filter efficiency at time t into the cycle, $\eta_c(t)$ and $\eta_s(t)$ are the efficiencies of the suspended particle cake and the sand bed during the last time increment, respectively.

Both of these terms, therefore, represent their respective efficiencies at time t into the filtration cycle.

In addition to the level of filter efficiency at time t, the average efficiency from the start of the filtration cycle to time t is of interest. This variable is calculated by accumulating the incremental efficiencies and then dividing by the number of increments. It is apparent that, unless floc breakthrough occurs, the filter efficiency will increase as a function of time. For this reason the average cycle efficiency will always be less than the current efficiency at time t.

Equation sequence 1 through 27 is repeated for the time increments until the desired time (or pressure drop) for filter backwash is reached. This time may well be determined by a trial-and-error method to facilitate filter operation between a residual pressure drop and some maximum desired pressure drop that allows the most economical operation of the filtration system.

It would be extremely difficult to perform these manipulations manually. This sequence is complex in that it considers many filter design parameters that are not normally taken into account in more classical design sequences. Because use of the digital computer has become widespread, application of complex concepts and lengthy design sequences, previously unused because of their arduous nature, can be easily accomplished; such is the case with this design technique for sand filtration systems. Since the design engineer can interact with the computer in the time-sharing mode he can consider a multitude of different concepts that were previously too complex or too time consuming for evaluation.

REFERENCES

1. Baylis, J. "Design Criteria for Rapid Sand Filters Journal, American Water Works Association, 51:11:1443, 1959.

2. Camp, I. "Theory of Water Filtration," American Society of Civil Engineers - Sanitary Engineering Division Journal, 90: SA4:1, 1964.

3. Carman, P. "Fluid Flow Through Granular Beds," Transactions of the Institute of Chemical Engineers (London, England), 15:150, 1937.

4. Cleasby, J. and F. Baumann. "Selection of Optimum Filtration Rates for Sand Filters," Progress Report, Project 380-S, Iowa Engineering Experimentation Station, Ames, Iowa, 1961.

5. Cleasby, J. and E. Baumann. "Selection of Sand Filtration Rates," Journal, American Water Works Association, 54:5:579, 1962.

6. Ives, K. and I. Sholji. "Research on Variables Affecting Filtration," American Society of Civil Engineers - Sanitary Engineering Division Journal, 91:SA4, Proc. 4436:1, 1965.

7. Yoder, R. and F. Empson. "The Effectiveness of Sand as a Filter Medium," Industrial Hygiene Journal, 107, April 1959.

8. Jacobs, S. "The Distribution of Pore Diameters in Graded Filters," Filtration and Separation (Great Britain), 9:525, 1972.

9. Grace, H. "Resistance and Compressibility of Filter Cakes," Chemical Engineering Progress, 49:6:303, 1953.

10. Chen, C. "Filtration of Aerosols by Fibrous Media," Chemical Review, 55:595, 1955.

11. Fuchs, N.A. The Mechanics of Aerosols. New York: Pergamon Press, 1964.

12. Friedlander, S. "Theory of Aerosol Filtration," Journal Industrial and Engineering Chemistry, 50:8:1161, 1958.

13. Friedlander, S. and R. Pascari. "The Efficiency of Fibrous Aerosol Filters," The Canadian Journal of Chemical Engineers, p. 212, December 1960.

14. Deb, A. "Discussion," Proceedings, American Society of Civil Engineers - Sanitary Engineering Division, 91:SA2 Proc. 4281:84, 1965.

15. Deb, A. "Discussion," Proceedings, American Society of Civil Engineers - Sanitary Engineering Division, 93:SA1 Proc. 4637:321, 1966.

16. Deb, A. "Discussion," Proceedings, American Society of Civil Engineers - Sanitary Engineering Division, 93:SA4 Proc. 5358:124, 1967.

17. Deb, A. "Theory of Sand Filtration," American Society of Civil Engineers, Sanitary Engineering Journal, 95:SA3:399, 1969.

18. Grace, H. "Structure and Performance of Filter Media," Journal, American Institute of Chemical Engineers, 2:3:307, 1956.

19. Hazen, R. "Elements of Filter Design," Journal, American Water Works Association, 43:3:208, 1951.

20. Ives, K. "Rational Design of Filters," Proceedings, Institute of Civil Engineers (London), 16:180, 1960.

21. Ives, K. "New Concepts in Filtration," Journal of Water and Wastewater Engineering, 65:307, 1961.

22. Ives, K. "Simplified Rational Analysis of Filter Behavior," Proceedings, Institute of Civil Engineers (London), 25:345, 1963.

23. Ives, K. "Progress in Filtration," Journal, American Water Works Association, 56:9:1226, 1964.

24. Ives, K. and J. Gregory. "Surface Forces in Filtration," Proceedings, Society of Water Treatment and Examination, 15:92, 1966.

INITIAL DISTRIBUTION

Hq USAF/PREE	1
Hq USAF/PREVP	1
Hq USAF/PREVX	1
Hq USAF/RDPS	2
Hq USAF/SAFOI	1
Hq USAF/SGPA	2
AFLC/SGB	1
AFLC/MAUT	1
AFSC/DE	1
AFFDL/TST	1
AFML/DO (Library)	1
OEHL/OL-AA	1
AFWL/SUL (Tech Library)	1
USAF SAM/EDE	2
FTD/LGM	1
AFIT/DEM	1
AU/LDG	1
AFSC/DEV	1
AFSC/SGB	1
AFSC/SGPE	1
AFSC/DLCAM	2
ATC/DEPV	1
Hq COMD/USAF/DEE	1
AFLC/DEPV	1
AFLC/MMRF	1
AFSC/SD	1
AMRL/DAL	1
OEHL/CC	3
OEHL/OL-AB	1
AFGL/XOP	1
AFRPL/Library	1
AMRL/THE	1
ASD/ENAMC	1
ASD/ENESS	1
AUL	1
AU/Surgeon	1
AFOSR	1
AFAPL	1
AEDC/DEE	1
SMASO/DEC	1
AMD/RDU	1
ARPA	1
ADTC/DLODL	1
OASD/(I&L)ES	1
Dir, USA WW Exp Stn	1
Dept of the Army/DARD-ARE-E	1
Dir, USA Eng R&D Lab/MERDC	1
AFRCE/Eastern Region	1
Naval Air Dev Ctr/MAE	1
ASD/ENFPA	1
ASD/DEP	1
ASD/SMKF	1
AFAL/TSR	1
SAMTEC/SEH	1
DDC/TCA	12
ADTC/CSV	1
Def Rsch & Engr/AD	1
USA Environ Hygn Agcy	1
Ch of Engr/ENGMC-RD	1
USA CERL	1
Ch of Naval Ops/Environ Protection Div	1
NCEL, Code 25111	1
AFRCE/Central Region	1
Naval Ship R&D Ctr/Code 3021	1
AFRCE/Western Region	1
Technology Transfer Staff (EPA)	1
Tech Application Ctr/Univ of NM	1
CEEDO/PRT	1
CEEDO/CC	1
National Science Found	1
US Army Med Bioengr R&D Lab	1
Office of R&D (EPA)	1
CEEDO/WE	1
CEEDO/EC	3